Dual-Chirp Microwave Waveform Generation Using a Dual-Parallel Mach–Zehnder Modulator

Dan Zhu, *Member, IEEE*, and Jianping Yao, *Fellow, IEEE*

***Abstract*— A photonic approach to generating a dual-chirp microwave waveform using a single dual-parallel Mach–Zehnder modulator (DPMZM) is proposed and experimentally demonstrated. A dual-chirp microwave waveform can be used in a radar system to improve its range-Doppler resolution. In the proposed approach, a baseband single-chirp waveform is applied to one sub-Mach–Zehnder modulator (sub-MZM) in the DPMZM and a microwave carrier is applied to the other sub-MZM. By biasing the two sub-MZMs at the minimum transmission point to suppress the optical carrier, a dual-chirp microwave waveform with a central frequency upconverted to the frequency of the microwave carrier is generated. A theoretical analysis is performed, which is then verified by a proof-of-concept experiment. A dual-chirp microwave waveform at 6 GHz with a tunable bandwidth at 200 MHz and 2 GHz is generated.**

***Index Terms*— Dual-chirp, linear frequency-modulated microwave waveform, microwave photonics, radar, range-Doppler coupling.**

I. Introduction

LINEAR frequency-modulated microwave waveforms, also known as linearly chirped microwave waveforms, have been widely used in radar systems to increase the range resolution through pulse compression [1], [2]. A linearly chirped microwave waveform, however, has a knife-edge-type ambiguity function [2] with large range-Doppler coupling, which would lead to a reduced range-Doppler resolution [1], [3]. A dual-chirp microwave waveform, on the other hand, has much smaller range-Doppler coupling and has been researched for use in radar systems to increase the range-Doppler resolution. A dual-chirp microwave waveform consists of two complementarily chirped microwave waveforms within the same time duration, with one having an up-chirp and the other a down-chirp [4]–[6]. In general, linearly chirped microwave waveforms can be generated electronically using either analog or digital circuits [7]–[11]. However, the central frequency and the bandwidth are usually limited to a few GHz. On the other hand, linearly chirped microwave waveforms can also be generated based on photonics, with a much higher central frequency and wider bandwidth thanks to the wide bandwidth offered by modern photonics. Numerous approaches have been proposed [12], [13]. For example, a linearly chirped microwave waveform can be generated based on spectral-shaping and wavelength-to-time mapping [12], but the chirp rate and the center frequency are usually fixed due to the fixed spectral response of the optical spectral shaper in the system, or a large number of switchable optical spectral shapers are needed at the cost of increased system complexity [13]. In addition, to reduce the range-Doppler coupling and to increase the range-Doppler resolution, a dual-chirp microwave waveform should be used. The generation of such a waveform based on photonics has not yet been reported.

In this letter, we propose and experimentally demonstrate a photonic approach to generating a dual-chirp microwave waveform using a single dual-parallel Mach-Zehnder modulator (DPMZM). A DPMZM has a Mach-Zehnder interferometer (MZI) structure with one sub-MZM (sub-MZM1) incorporated in the upper arm and a second sub-MZM (sub-MZM2) in the lower arm. A phase modulator (PM) is also incorporated in the lower arm after the sub-MZM2. A microwave carrier and a baseband single-chirp waveform are applied to the two sub-MZMs, and the sub-MZMs are both biased at the minimum transmission point to achieve carrier-suppressed modulation. The modulated signal from sub-MZM2 is combined with the modulated signal from sub-MZM1, and then applied to a photodetector (PD). A dual-chirp microwave waveform is thus generated at the output of the PD. The key advantage of the approach is that two functions using a single DPMZM are implemented simultaneously, 1) to generate two complementarily chirped microwave waveforms, and 2) to up-convert the central frequency of the dual-chirp microwave waveform to the frequency of the microwave carrier. The proposed approach is theoretically analyzed and experimentally demonstrated. A dual-chirp microwave waveform at 6 GHz with a bandwidth tunable at 200 MHz and 2 GHz is generated. The use of the generated dual-chirp waveform to overcome the range-Doppler coupling effect is also analyzed and discussed.

II. Principle

The schematic of the proposed dual-chirp microwave waveform generation system based on a single DPMZM is shown in Fig. 1. A light wave at ω_0 generated by

Manuscript received February 5, 2015; revised March 29, 2015; accepted April 12, 2015. Date of publication April 14, 2015; date of current version June 9, 2015. This work was supported by the Natural Science and Engineering Research Council of Canada. The work of D. Zhu was supported by the China Scholarship Council.

D. Zhu is with the Microwave Photonics Research Laboratory, School of Electrical Engineering and Computer Science, University of Ottawa, Ottawa, ON K1N 6N5, Canada, and also with the College of Electronic and Information Engineering, Nanjing University of Aeronautics and Astronautics, Nanjing 210016, China.

J. Yao is with the Microwave Photonics Research Laboratory, School of Electrical Engineering and Computer Science, University of Ottawa, Ottawa, ON K1N 6N5, Canada (e-mail: jpyao@eecs.uottawa.ca).

Color versions of one or more of the figures in this letter are available online at http://ieeexplore.ieee.org.

Digital Object Identifier 10.1109/LPT.2015.2422812

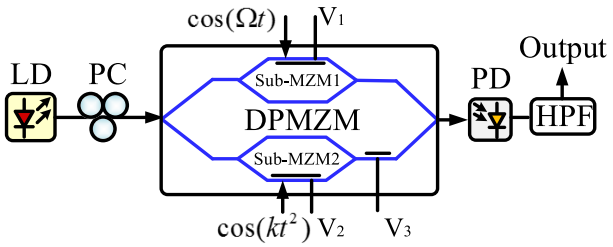

Fig. 1. The schematic of the proposed dual-chirp microwave waveform generation system based on a single DPMZM. LD: laser diode; PC: polarization controller; LFM: linear frequency modulated; DPMZM: dual parallel Mach-Zehnder modulator; PD: photodetector; HPF: high pass filter.

a laser diode (LD) is sent to a DPMZM via a polarization controller (PC). The DPMZM consists of two sub-MZMs (sub-MZM1 and sub-MZM2) with one in the upper arm and the other in the lower arm. A PM is also incorporated in the lower arm. The two sub-MZMs are both biased at the minimum transmission point to achieve carrier-suppression modulation. In the system, a microwave carrier $\cos(\Omega t)$ with a frequency at Ω and a baseband single-chirp waveform $\cos(kt^2)$ with a chirp rate of k are applied to sub-MZM1 and sub-MZM2, respectively. The optical signal at the output of the DPMZM is given by

$$E(t) = E_o e^{j\omega_0 t} \times \left[e^{j\beta_1 \cos(\Omega t)} + e^{j\beta_2 \cos(kt^2)} \cdot e^{j\phi_3} \right] \quad (1)$$

where E_0 is the amplitude of the optical field, $\beta_i = \pi V_i / V_{\pi i}$ $(i = 1, 2)$, V_i is the amplitude of the signals applied to sub-MZM$_i$, $V_{\pi i}$ is the half-wave voltage of sub-MZM$_i$. ϕ_3 is a static phase introduced by the PM with a bias voltage V_3 to the modulated optical signal from sub-MZM2. Under small-signal modulation condition, by applying the Jacobi-Anger expansion to (1) and considering the carrier-suppressed bias condition in the sub-MZMs, we have

$$\begin{aligned} E(t) = {} & J_1(\beta_1) e^{j(\omega_0 - \Omega)t} + J_1(\beta_1) e^{j(\omega_0 + \Omega)t} \\ & + J_1(\beta_2) e^{j(\omega_0 t - kt^2 + \phi_3)} + J_1(\beta_2) e^{j(\omega_0 t + kt^2 + \phi_3)} \end{aligned} \quad (2)$$

where $J_n (n = 1, 2)$ is the n^{th}-order Bessel function of the first kind. By introducing the signal in (2) into a PD, the AC term of the output electrical signal is given by

$$\begin{aligned} i_o(t) \propto {} & 2J_1^2(\beta_1) \cos\left(2kt^2\right) + 2J_1^2(\beta_2) \cos(2\Omega t) \\ & + 4J_1(\beta_1) J_1(\beta_2) \cos(\phi_3) \cos\left(\Omega t + kt^2\right) \\ & + 4J_1(\beta_1) J_1(\beta_2) \cos(\phi_3) \cos\left(\Omega t - kt^2\right) \end{aligned} \quad (3)$$

The high-frequency term $\cos(2\Omega t)$ is eliminated due to the bandwidth-limited nature of the PD. By removing the low-frequency term $\cos(2kt^2)$ using an electrical high-pass filter (HPF), the output microwave current will be

$$\begin{aligned} i_o(t) \propto {} & 4J_1(\beta_1) J_1(\beta_2) \cos(\phi_3) \\ & \times \left[\cos\left(\Omega t + kt^2\right) + \cos\left(\Omega t - kt^2\right) \right] \end{aligned} \quad (4)$$

As can be seen from (4), a dual-chirp microwave waveform centered at the frequency of Ω is generated. By setting the bias V_3 to make $\phi_3 = 0$, the generated dual-chirp microwave waveform will have the largest amplitude. By tuning the frequency Ω of the microwave signal applied to sub-MZM1, the central frequency of the dual-chirp microwave waveform can be tuned. In addition, by tuning the value k of the base-band single-chirp waveform $\cos(kt^2)$ applied to sub-MZM2, the chirp rate and bandwidth of the dual-chirp microwave waveform can also be tuned.

The use of a dual-chirp microwave waveform in a radar system will increase the range-Doppler resolution. The range-Doppler resolution is evaluated by the ambiguity function given by [2],

$$\left| \chi(\tau, \Omega_d) \right|^2 = \left| \int_{-\infty}^{+\infty} i(t)\, i^*(t - \tau) e^{j\Omega_d t} dt \right|^2 \quad (5)$$

where τ and Ω_d are the time delay and frequency shift which represent the range of a target and its radial velocity, respectively.

For a single-chirp microwave waveform given by

$$i_s(t) = \frac{1}{\sqrt{T}} rect\left(\frac{t}{T}\right) e^{j(\Omega t \pm kt^2)} \quad (6)$$

where $rect(\xi) = \begin{cases} 1, & for\ |\xi| \le 0.5 \\ 0, & else \end{cases}$, T is the waveform time duration, and $\pm$ corresponds to an up and down-chirp waveform. The corresponding ambiguity function is given by

$$\begin{aligned} & \left| \chi_s(\tau, \Omega_d) \right|^2 \\ & = \left| \left(1 - \frac{|\tau|}{T}\right) \frac{\sin\left[\frac{1}{2}T\left(2k\tau \pm \Omega_d\right)\left(1 - \frac{|\tau|}{T}\right)\right]}{\frac{1}{2}T\left(2k\tau \pm \Omega_d\right)\left(1 - \frac{|\tau|}{T}\right)} \right|^2, \quad for\ |\tau| \le T \end{aligned} \quad (7)$$

This ambiguity function has a knife-edge shape, leading to a large range-Doppler coupling with a reduced range-Doppler resolution [1].

For a dual-chirp microwave waveform, given by

$$i_d(t) = \frac{\sqrt{2}}{2} \frac{1}{\sqrt{T}} Rect\left(\frac{t}{T}\right) \left[e^{j(\Omega t + kt^2)} + e^{j(\Omega t - kt^2)} \right] \quad (8)$$

Its ambiguity function is given by

$$\begin{aligned} & \left| \chi_d(\tau, \Omega_d) \right|^2 \\ & = \frac{1}{4} \times \left| \left(1 - \frac{|\tau|}{T}\right) \frac{\sin\left[\frac{1}{2}T\left(2k\tau + \Omega_d\right)\left(1 - \frac{|\tau|}{T}\right)\right]}{\frac{1}{2}T\left(2k\tau + \Omega_d\right)\left(1 - \frac{|\tau|}{T}\right)} \right. \\ & \quad \left. + \left(1 - \frac{|\tau|}{T}\right) \frac{\sin\left[\frac{1}{2}T\left(2k\tau - \Omega_d\right)\left(1 - \frac{|\tau|}{T}\right)\right]}{\frac{1}{2}T\left(2k\tau - \Omega_d\right)\left(1 - \frac{|\tau|}{T}\right)} \right|^2, \\ & \quad for\ |\tau| \le T \end{aligned} \quad (9)$$

As can be seen, the ambiguity function is a combination of two Sinc functions with the peaks of the functions located at the origin, while the sidelobes at different locations. The mainlobe at the origin is maintained unchanged while the sidelobes are decreased by 4 times, which would lead to a decrease in the −3-dB contour of the ambiguity function [2]. Thus, the range-Doppler coupling is reduced and the range-Doppler resolution is improved.

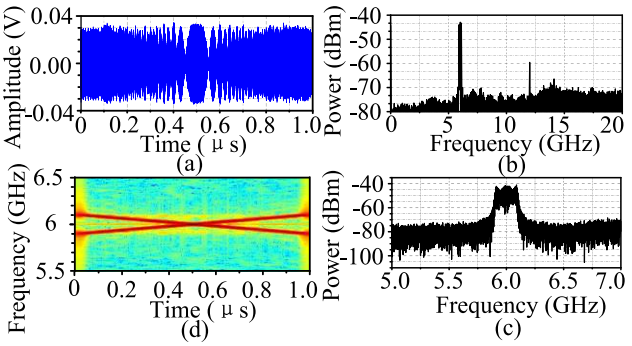

Fig. 2. (a) The generated dual-chirp microwave waveform with a 200-MHz bandwidth centered at 6 GHz, (b) the electrical spectrum with a 20-GHz span, (c) the electrical spectrum with a 2-GHz span, and (d) the instantaneous frequency-time diagram of the generated dual-chirp microwave waveform.

III. Experimental Results and Disscussion

An experiment based on the setup shown in Fig. 1 is carried out. A light wave at 1550 nm from the LD (Agilent N7714A) is sent to the DPMZM (JDSU 470661H) through the PC. The DPMZM has a bandwidth of 10 GHz. The microwave carrier and the baseband chirped waveform applied to sub-MZM1 and sub-MZM2 are generated by a microwave signal generator (Agilent E8254A) and an arbitrary waveform generator (AWG, Tektronix AWG7102, 10 GS/s), respectively. The optical signal from the DPMZM is sent to the PD (NEWFOCUS 10058B) which has a bandwidth of 20 GHz. The detected signal is sent to the electrical BPF with a bandwidth of 4 GHz from 4 to 8 GHz to filter out the lower frequency term. The electrical spectrum of the generated dual-chirp microwave waveform is observed by an electrical spectrum analyzer (Agilent E4448A). The temporal waveform is monitored by a digital storage oscilloscope (Agilent DSO-X 93204A). In the experiment, a 10-dBm 6-GHz microwave signal is applied to sub-MZM1, and a baseband chirp signal with time duration of 1 μs is applied to sub-MZM2. The bias voltages to sub-MZM1, sub-MZM2 and the PM are set at 7.2 V, 6.5 V and 1.2 V, respectively.

A dual-chip microwave waveform is then generated. Note the value k in the baseband chirped waveform is set at $\pi \times 10^{14}$ s^{-2}. The waveform generated by the electrical AWG in our experiment is periodic. The generated dual-chirp waveform is also periodic. The temporal waveform (one period) and its spectrum (with a span from 0 to 20 GHz) are shown in Fig. 2(a) and (b), respectively. Fig. 2(c) provides a zoom-in view of the spectrum at around 6 GHz. As can be seen a dual-chirp microwave waveform with time duration of 1 μs and bandwidth of 200 MHz centered at 6 GHz is generated. The instantaneous frequency-time diagram for the waveform is shown in Fig. 2(d), which confirms that a dual-chirp microwave waveform consisting of an up-chirp (with an instantaneous frequency from 5.9 to 6.1 GHz) and a down-chirp waveform (with an instantaneous frequency from 6.1 to 5.9 GHz) is realized.

Fig. 3(a) and (b) shows the ambiguity function of the generated dual-chirp microwave waveform and the corresponding contour map. As a comparison, the ambiguity functions for a simulated single up- and down-chirp microwave waveform with the same bandwidth of 200 MHz

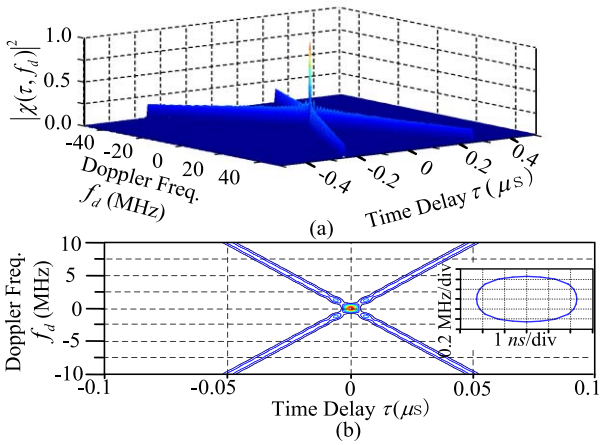

Fig. 3. (a) The ambiguity function and (b) the corresponding contour map for the generated dual-chirp microwave waveform with a 200-MHz bandwidth centered at 6 GHz, Inset: the −3-dB contour map.

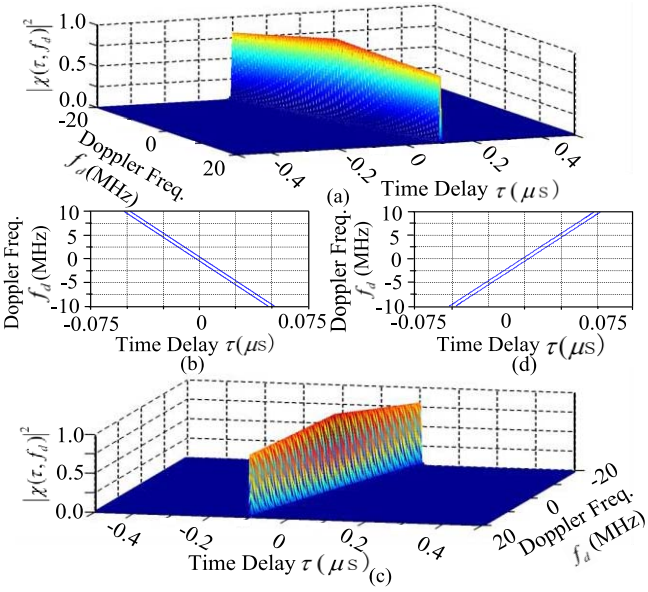

Fig. 4. (a) The ambiguity function and (b) the −3-dB contour map for the simulated single down-chirp microwave waveform with a 200-MHz bandwidth centered at 6 GHz; (c) the ambiguity function and (d) the −3-dB counter map for the simulated single up-chirp microwave waveform with a 200-MHz bandwidth centered at 6 GHz.

and central frequency of 6 GHz are shown in Fig. 4. As can be seen, both the ambiguity functions for a single up- and down-chirp microwave waveform have a knife-edge ambiguity function [1], and the −3-dB contour maps, shown in Fig. 4(b) and (d), are much greater than that shown in the insert of Fig. 3(b). Thus, it is verified that the use of a dual-chirp microwave waveform will increase the range-Doppler resolution in a radar system.

The bandwidth of the dual-chirp waveform can be tuned by tuning the chirp rate of the baseband single-chirp waveform. In the experiment, by setting the value k in the baseband chirp waveform to be $\pi \times 10^{15}$ s^{-2}, a dual-chirp microwave waveform with a bandwidth of 2 GHz is generated. The temporal waveform and the electrical spectrum are shown in Fig. 5(a) and (b). Fig. 5(c) is a zoom-in view of the spectrum around 6 GHz. As can be seen a dual-chirp microwave

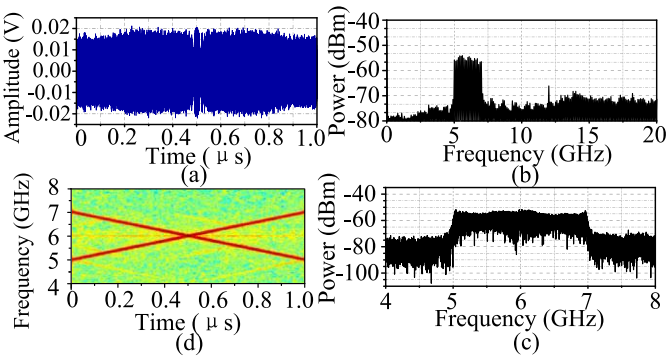

Fig. 5. (a) The waveform, (b) the electrical spectrum with 20-GHz span and (c) 2-GHz span, and (d) the instantaneous frequency-time diagram of the generated dual-chirp microwave waveform with 2-GHz bandwidth centered at 6 GHz.

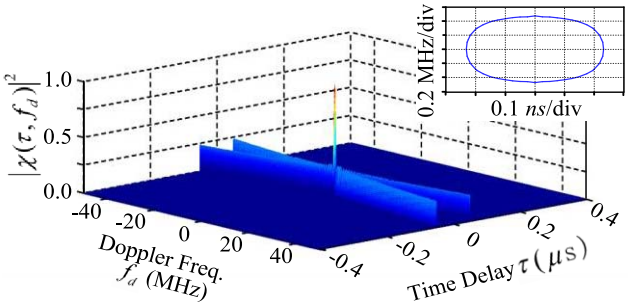

Fig. 6. The ambiguity function of the generated 1-μs dual-chirp microwave waveform with a 2-GHz bandwidth centered at 6 GHz. Inset: the −3-dB contour map of the ambiguity function.

waveform with time duration of 1 μs and a bandwidth of 2 GHz centered at 6 GHz is generated. The instantaneous frequency-time diagram for the waveform is shown in Fig. 5(d), which confirms that a dual-chirp microwave waveform consisting of an up-chirp (with an instantaneous frequency from 5 to 7 GHz) and a down-chirp microwave waveform (with an instantaneous frequency from 7 to 5 GHz) is realized.

The ambiguity function of the generated dual-chirp microwave waveform with a 2-GHz bandwidth is also analyzed, with the results shown in Fig. 6. As can be seen, the main-to-sidelobe ratio is improved and the −3-dB contour is significantly decreased. By comparing the −3-dB contour map with that for the waveform with a 200-MHz bandwidth, we can see that the value of the point of the −3-dB contour map located on the axis of the time delay is decreased by 10 times, while that located on the axis of the Doppler frequency keeps the same, thus the −3-dB contour map is decreased by 10 times for the waveform with a 2-GHz bandwidth, which indicates that a wider bandwidth will have a better range-Doppler resolution.

IV. Discussion and Conclusion

Because of the limited bandwidth of the DPMZM used in the experiment, the generated dual-chirp microwave waveform had a central frequency of 6 GHz and a maximum bandwidth of 2 GHz. If a DPMZM and a PD with a wider bandwidth are used, the generated dual-chirp microwave waveform would have a much higher central frequency and wider bandwidth. Of course, the maximum bandwidth and central frequency is also determined by the electrical AWG used to generate the baseband single-chirp waveform. In addition, the temporal duration of the baseband waveform can be controlled long, thus a dual-chirp microwave waveform with a large time bandwidth product (TBWP) can be generated.

In conclusion, we have proposed and experimentally demonstrated a photonic approach to generating a dual-chirp microwave waveform using a single DPMZM. The key contribution of the work is the use of a single DPMZM to perform two functions simultaneously, to generate a dual-chirp microwave waveform and to up-convert the central frequency of the dual-chirp waveform to that of the microwave carrier. The proposed technique was experimentally evaluated. A dual-chirp microwave waveform centered at 6 GHz with a temporal duration of 1 μs and a bandwidth of 200 MHz and 2 GHz was generated. Compared with a single-chirp microwave waveform, the range-Doppler resolution was significantly increased. Since the dual-chirp microwave waveform was generated in the optical domain, the technique can be used in a distributed radar system in which microwave waveforms are distributed over optical fibers to take advantage of the ultra-broad bandwidth and low loss of modern photonics technology [14], [15].

References

[1] M. A. Richards, *Fundamentals of Radar Signal Processing*, 2nd ed. New York, NY, USA: McGraw-Hill, 2014.
[2] M. I. Skolnik, *Introduction to Radar Systems*, 2nd ed. New York, NY, USA: McGraw-Hill, 2001.
[3] R. J. Fitzgerald, "Effects of range-doppler coupling on chirp radar tracking accuracy," *IEEE Trans. Aerosp. Electron. Syst.*, vol. AES-10, no. 4, pp. 528–532, Jul. 1974.
[4] A. Amar and Y. Buchris, "Asynchronous transmitter position and velocity estimation using a dual linear chirp," *IEEE Signal Process. Lett.*, vol. 21, no. 9, pp. 1078–1082, Sep. 2014.
[5] A. A. Dotan and I. Rusnak, "Method of measuring closing velocity by transmitting a dual-chirp signal," in *Proc. 26th IEEE Conf. Elect. Electron. Eng. Israel*, Eilat, Israel, Nov. 2010, pp. 000258–000262.
[6] K. Iwashita, T. Moriya, N. Tagawa, and M. Yoshizawa, "Doppler measurement using a pair of FM-chirp signals," in *Proc. IEEE Symp. Ultrason.*, Honolulu, HI, USA, Oct. 2003, pp. 1219–1222.
[7] R. J. C. Middleton, D. G. Macfarlane, and D. A. Robertson, "Range autofocus for linearly frequency-modulated continuous wave radar," *IET Radar, Sonar Navigat.*, vol. 5, no. 3, pp. 288–295, Mar. 2011.
[8] R. Weigel *et al.*, "Microwave acoustic materials, devices, and applications," *IEEE Trans. Microw. Theory Techn.*, vol. 50, no. 3, pp. 738–749, Mar. 2002.
[9] C. M. Panasik, "Multiple frequency acoustic reflector array and monolithic cover for resonators and method," U.S. Patent 6 441 703, Aug. 27, 2002.
[10] P. Symons, *Digital Waveform Generation*. New York, NY, USA: Cambridge Univ. Press, 2013.
[11] D. Gomez-Garcia, C. Leuschen, F. Rodriguez-Morales, J.-B. Yan, and P. Gogineni, "Linear chirp generator based on direct digital synthesis and frequency multiplication for airborne FMCW snow probing radar," in *Proc. IEEE MTT-S Int. Microw. Symp. (IMS)*, Tampa, FL, USA, Jun. 2014, pp. 1–4.
[12] J. Yao, "Photonic generation of microwave arbitrary waveforms," *Opt. Commun.*, vol. 284, no. 15, pp. 3723–3736, Jul. 2011.
[13] M. H. Khan *et al.*, "Ultrabroad-bandwidth arbitrary radiofrequency waveform generation with a silicon photonic chip-based spectral shaper," *Nature Photon.*, vol. 4, pp. 117–122, Feb. 2010.
[14] A. Kanno and T. Kawanishi, "Broadband frequency-modulated continuous-wave signal generation by optical modulation technique," *J. Lightw. Technol.*, vol. 32, no. 20, pp. 3566–3572, Oct. 15, 2014.
[15] T. Yao, D. Zhu, S. Liu, F. Zhang, and S. Pan, "Wavelength-division multiplexed fiber-connected sensor network for source localization," *IEEE Photon. Technol. Lett.*, vol. 26, no. 18, pp. 1874–1877, Sep. 15, 2014.